

Searching for Active Latitudes Using Transiting Exoplanets

JAMES. R. A. DAVENPORT,^{1,*} BRETT M. MORRIS,¹ LESLIE HEBB,² MICHELLE GOMEZ,² ERIC AGOL,¹
AND SUZANNE L. HAWLEY¹

¹*Department of Astronomy, University of Washington, Seattle, WA 98195, USA*

²*Department of Physics, Hobart and William Smith Colleges, Geneva, NY, 14456*

ABSTRACT

Active latitude bands, as well as the “Solar Butterfly Diagram”, are foundational properties that drive models of the solar dynamo. However, while considerable progress has been made on modeling stellar dynamos, no comparable constraint for the latitude distribution of active regions has been available. Here we present an ensemble approach to studying the latitude distribution of starspots using *Kepler* transiting exoplanets. By exploiting the differences in impact parameter (b), the planets occult a range of latitude bands. We find X, using Y stars, and note Z. The future is bright.

Keywords: stars: activity

1. INTRODUCTION

The latitude range over which sunspots form throughout the course of the solar activity cycle is a key observable constraint in stellar dynamo theory. Spots trace the local surface magnetic field, and are therefore valuable for understanding the geometry and strength of a star’s internal magnetic field (Berdyugina 2005). For the Sun, spots predominantly form within two roughly symmetric bands of latitude centered about the equator. Throughout the ~ 11 year solar activity cycle, the mean latitudes of these bands decreases towards the equator, from $\sim 30^\circ$ to $\sim 5^\circ$ (e.g. see ?). This sunspot latitude variation over time is known as the “Spörer’s Law” (or colloquially as the Butterfly diagram), and was first summarized by Maunder (1904).

“Active latitudes” as observed on the Sun occur naturally as a result of both stellar rotation and differential rotation, which together govern

the activity cycle length in the $\alpha\Omega$ mean-field dynamo model (Brandenburg & Subramanian 2005). The rate of stellar mass and angular momentum loss over time is also dependent on the surface magnetic field morphology (Garraffo et al. 2015), and improvements in stellar spin-down models will require advances in surface magnetic field maps (Garraffo et al. 2016). Determining the latitudes of starspots is therefore vital for calibrating mean field dynamo theory from the Sun to other stars.

Much work has been done to search for other observable constraints of Solar-like dynamo activity in other stars. Considerable effort has been made to search for overall magnetic activity cycles for stars, primarily in measuring chromospheric Ca II H&K emission over many decades (Wilson 1978; Baliunas et al. 1995, e.g.). These surveys require long observation baselines, and have yielded many potential activity cycle detections from samples of hundreds of nearby stars. Starspot-modulation rotation curves have been measured for tens of

* DIRAC Fellow

thousands of stars using space-based photometric monitoring (McQuillan et al. 2014), providing evidence of stellar dynamos producing surface spots. Differential rotation constraints using starspot modulation curves has been attempted (e.g. Reinhold et al. 2013), but remains effectively unconstrained due to degeneracies between spot evolution and differential rotation (Aigrain et al. 2015). A few notable exceptions have been found for rapidly rotating stars with slowly evolving, long-lived spots (e.g. Morin et al. 2008; Davenport et al. 2015), but these are likely due to polar starspots that represent non-Solar dynamo type activity.

Despite its importance, starspot latitudes have only been constrained for a handful of systems. Coarse maps of the stellar magnetic field can be generated via Doppler Imaging techniques for rapidly rotating stars (Semel 1989; Donati & Brown 1997), but typically cannot resolve small enough size scales to study individual spots comparable to those observed on the Sun. For a small number of nearby active stars, the surface can be imaged directly via interferometry. Roettenbacher et al. (2016) made use of this method to map the starspots on the old active star, ζ And, finding no sign of a solar-like spot distribution. Techniques for constraining starspot latitudes for larger samples of stars, particularly for older or slower rotating stars, are desperately needed.

Here we introduce a statistical approach to mapping the distribution of starspots as a function of stellar latitude for stars with a transiting exoplanet. Transiting exoplanets have been previously used to probe the starspot activity along single latitude bands for individual stars (e.g. Morris et al. 2017). By exploiting the varying geometry for many transiting systems, specifically the impact parameter, we seek to create an ensemble portrait of the latitudes where starspots are most prevalent. While the detailed geometry of each transiting planet+star system

requires careful consideration to correctly map observed features back to precise stellar latitudes, the method can in principle be applied to characterize a great number of transit host stars. This approach can be extended beyond single-band transit photometry, which will help measure detailed active region properties, and with extended monitoring campaigns of transits we may be able to simultaneously model the stellar activity cycles.

2. STARSPOT PROPERTIES FROM TRANSIT TOMOGRAPHY

Transiting exoplanets provide a unique means to detect small-scale surface features on stars. As the planet passes in front of the star, changing levels of flux on the stellar surface due to hot or cool regions affect the transit depth. In this “transit tomography”, the planet provides a one-dimensional map of the surface brightness. When the planet passes over cool starspots, the transit depth is briefly shallower, resulting in “bumps” in the transit light curve (Silva 2003). The resulting amplitude of these bumps are determined by the planet size relative to the star (which governs the overall transit depth), the starspot size relative to the planet, and the temperature contrast of the spot to the average photosphere. For bright, nearby stars with transiting Neptune or Jupiter sized planets, these bumps can reach $\sim 1/4$ the transit depth.

The most informative scenario for determining starspot latitudes occurs when the stellar rotation and planetary orbital axes are significantly misaligned, as is the case for Hat-P-11 (Sanchis-Ojeda & Winn 2011). In this geometry, the planet passes in front of the star in a nearly orthogonal direction to the rotation axis, mapping out a range of latitudes with each transit. For Hat-P-11, two distinct active latitude bands have been discovered, which reveal a solar-like dynamo at work (Morris et al. 2017). However, for most transiting systems the planetary orbit and stellar spin axes are well aligned,

resulting in a fixed range of latitudes sampled by every transit, as in the Kepler 17 system (Davenport 2015). Transiting multi-planet systems may provide another means to study a range of latitudes for a single star (e.g. Kepler 186; Quintana et al. 2014), but the sample of such systems is currently quite small.

Missions like *Kepler* now routinely observe transits with the photometric precision required to detect these bumps (Borucki et al. 2010), and indeed many *Kepler* systems have had their spot properties measured from this technique (e.g. Sanchis-Ojeda & Winn 2011; Sanchis-Ojeda et al. 2013). In the best cases, for bright stars and with 1-minute cadence, hundreds of individual starspots have been detected (e.g. Davenport 2015), and fit with detailed forwarding modeling (Hebb et al. in prep). However, many transiting systems in *Kepler* are either too faint, or have too slow of an observing cadence (30-minute), to resolve individual starspot bumps. For these fainter stars the transit signature may still be impacted by starspot crossings, with the transit depth or even duration appearing variable when monitoring for many transits.

Naturally, to detect a starspot bump in transit the transit chord projected onto the star must intersect regions on the surface containing starspots. In Figure 1 we demonstrate three identical transiting exoplanets with differing impact parameters, whose transits project onto different ranges in latitude on the star. The starspots are placed at typical latitudes for those found on the Sun, centered at $\sim 25^\circ$ latitude. In this case, the intermediate transit (planet B) with an impact factor of $b = 0.5$ intersects the northern active latitude of the star.

As we combine lots of transits, we get lots of scatter in vs out of transit! show example from Kepler17

Now lets use LOTS of transits, but vary the impact parameter

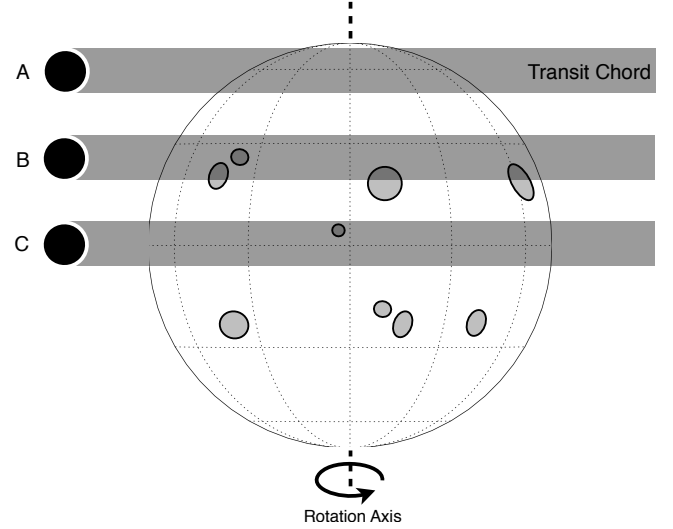


Figure 1. Schematic diagram of star with active starspot latitudes centered at $\sim 25^\circ$ latitude, and three transiting exoplanets with impact parameters ranging between nearly $b=1$ (A) to $b=0$ (C). The planet size is typical of a hot Jupiter, with $r_p/r_\star \sim 0.11$.

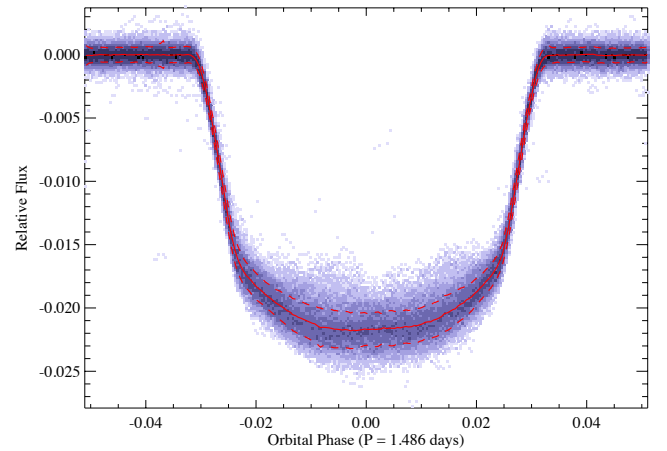


Figure 2. Overlay of every short-cadence *Kepler* transit for Kepler 17 from Davenport (2015). Starspot variations have been normalized out using second-order polynomial fits to the out-of-transit regions. The binned median (solid line) and standard deviation (dashed line) show that the in-transit scatter due to starspot crossings is ~ 2.5 larger than the out-of-transit scatter due primarily to photometric noise.

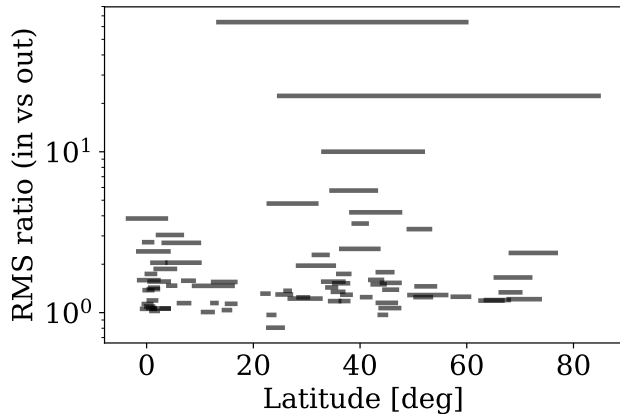


Figure 3. the real data – its kinda rough, but sample size small...

note: a uniform distribution of impact parameters does NOT result in a uniform mapping of

latitudes. hard to see high- B spots due to foreshortening.

3. ENSEMBLE SPOT LATITUDE MAPPING

4. *Kepler* TRANSITING SYSTEMS

we tried it with *Kepler*. It didn't work great, but we have a few thoughts as to why

5. SUMMARY

JRAD acknowledges support by an NSF Astronomy and Astrophysics Postdoctoral Fellowship under award AST-1501418.

REFERENCES

- Aigrain, S., Llama, J., Ceillier, T., et al. 2015, MNRAS, 450, 3211
- Baliunas, S. L., Donahue, R. A., Soon, W. H., et al. 1995, ApJ, 438, 269
- Berdugina, S. V. 2005, Living Reviews in Solar Physics, 2, 8
- Borucki, W. J., Koch, D., Basri, G., et al. 2010, Science, 327, 977
- Brandenburg, A., & Subramanian, K. 2005, PhR, 417, 1
- Davenport, J. R. A. 2015, PhD thesis, University of Washington, doi:10.5281/zenodo.47231
- Davenport, J. R. A., Hebb, L., & Hawley, S. L. 2015, ApJ, 806, 212
- Donati, J.-F., & Brown, S. F. 1997, A&A, 326, 1135
- Garraffo, C., Drake, J. J., & Cohen, O. 2015, ApJ, 813, 40
- . 2016, A&A, 595, A110
- Maunder, E. W. 1904, MNRAS, 64, 747
- McQuillan, A., Mazeh, T., & Aigrain, S. 2014, ApJS, 211, 24
- Morin, J., Donati, J.-F., Forveille, T., et al. 2008, MNRAS, 384, 77
- Morris, B. M., Hebb, L., Davenport, J. R. A., Rohn, G., & Hawley, S. L. 2017, ApJ, 846, 99
- Quintana, E. V., Barclay, T., Raymond, S. N., et al. 2014, Science, 344, 277
- Reinhold, T., Reiners, A., & Basri, G. 2013, A&A, 560, A4
- Roettenbacher, R. M., Monnier, J. D., Korhonen, H., et al. 2016, Nature, 533, 217
- Sanchis-Ojeda, R., & Winn, J. N. 2011, ApJ, 743, 61
- Sanchis-Ojeda, R., Winn, J. N., Marcy, G. W., et al. 2013, ApJ, 775, 54
- Semel, M. 1989, A&A, 225, 456
- Silva, A. V. R. 2003, ApJL, 585, L147
- Wilson, O. C. 1978, ApJ, 226, 379